American Mineralogist, Volume 89, pages 239–245, 2004

Novel phase transition in orthoenstatite

JENNIFER M. JACKSON,[1,]* STANISLAV V. SINOGEIKIN,[1] MICHAEL A. CARPENTER,[2] AND JAY D. BASS[1]

[1] Department of Geology, University of Illinois, Urbana, Illinois 61801, U.S.A.
[2] Department of Earth Sciences, University of Cambridge, Cambridge CB2 3EQ, U.K.

ABSTRACT

Single-crystal Brillouin scattering measurements on natural orthoenstatite [OEN] to 1350 °C at 1 atm show significant softening of the elastic moduli C_{33} and C_{55} ahead of a phase transition. To our knowledge, these are the first observations of acoustic mode-softening in orthoenstatite at high temperature and room pressure and could have important implications for Earth's mantle. The phase transition is rapid and shows some hysteresis in the observed transition temperature, T_{tr}. Experiments performed on increasing and decreasing temperature bracket the transition temperature between 1090(10) °C ≤ T_{tr} ≤ 1175(10) °C, and pronounced acoustic mode-softening is evident at temperatures above 900 °C. Backscattering measurements to T = 1350 °C show no evidence for additional transitions. OEN was recovered at room temperature. Our results are interpreted in terms of elastic softening ahead of a displacive phase transition. Before the displacive transition can occur, however, the elastic softening appears to trigger the observed reconstructive transition to the more-stable protoenstatite (or high clinoenstatite) structure. We suggest that the displacive phase transition would lead to a previously unreported pyroxene structure with *Cmca* symmetry.

INTRODUCTION

Orthopyroxene, $(Mg,Fe)_2Si_2O_6$, is an abundant mineral in mafic rocks of Earth's crust and upper mantle. Although the existence of several $Mg_2Si_2O_6$ polymorphs has been demonstrated from both laboratory experiments and natural occurrences, orthoenstatite (OEN, space group *Pbca*) is by far the most abundant (Deer et al. 1978). Low-clinoenstatite (LCE, $P2_1/c$) is rare in terrestrial rocks, being found in meteorites, in unusual volcanic rocks (Komatsu 1980; Shimbayashi and Kitamura 1991), and as fine scale intergrowths in OEN of igneous and metamorphic rocks (Bozhilov et al. 1999; Busek and Iijima 1975). High-pressure clinoenstatite (HPCE, $C2/c$) (Ross and Reynard 1999; Angel et al. 1992; Ulmer and Stalder 2001) is a non-quenchable high-pressure polymorph. Protoenstatite (PEN, *Pbcn*) (e.g., Jiang et al. 2002) and high-temperature clinoenstatite (HTCE, $C2/c$) (e.g., Shimobayashi and Kitamura 1993) have been reported as high-temperature (1 atm) polymorphs of $Mg_2Si_2O_6$, the latter being non-quenchable.

The high-temperature 1 atm phase relations of $Mg_2Si_2O_6$-pyroxene polymorphs are uncertain. Shimobayashi and Kitamura (1993) showed by high-temperature TEM analyses that OEN transforms to HTCE above ~1200 °C (1 atm), finding no evidence for PEN. However, several reports concluded that at 1 atm PEN is the only stable phase between ~1000 °C and the incongruent melting point of 1557 °C (e.g., Boyd et al. 1964; Murakami et al. 1982; Schrader et al. 1990; Boysen et al. 1991; Biggar 1992; Thiéblot et al. 1999; Jiang et al. 2002). These results are supported by molecular dynamics simulations (Matsui and Price 1992) and lattice dynamics calculations (Choudhury and Chaplot 2000; Choudhury et al. 1998), which suggest that OEN transforms to PEN, not HTCE, at high temperatures. Some studies indicate that both HTCE and PEN have high-temperature stability fields (Ernst and Schwab 1970; Iishi and Kitayama 1995). Intermediate phases also have been described near the transition (e.g., Schrader et al. 1990). Furthermore, the temperatures reported for the transition of OEN to a high-temperature phase ranges from 950 °C (Smyth 1971) to 1230 °C (Shimobayashi and Kitamura 1993). The conflicting results on the stabilities of the enstatite polymorphs have been explained by variations in sample chemistry (sometimes induced by fluxes), grain size, thermal history, microstructures, as well as the difficulty of accurately identifying different polymorphs by X-ray diffraction (XRD) (e.g., Sarver and Hummel 1962; Brown and Smith 1963; Sueno and Prewitt 1963). Regardless of which high-temperature polymorph is observed, the transition has been reported to be sluggish and partially reconstructive, requiring the breakage of Mg-O bonds (e.g., Smyth 1974a).

In the present study, we measured the acoustic properties of natural OEN in the temperature range from 20 to 1350 °C at 1 atm in an attempt to clarify the mechanism and transition temperature of OEN to a higher-temperature polymorph. Elastic softening was observed in OEN, and we propose that it can be understood in terms of strain coupling to the order parameter for a displacive phase transition to a new orthopyroxene structure with space group *Cmca*. Most unusually, this softening seems to trigger the observed reconstructive transition to the equilibrium high-temperature structure.

EXPERIMENTAL PROCEDURES

Colorless, euhedral single crystals of orthoenstatite from Zabargad Island, Egypt were used in this study (Kurat et al. 1993). The simplified chemical formula, as determined from electron microprobe analyses, is: $(Mg_{0.994}Fe_{0.002}Al_{0.004})_2(Si_{0.996}Al_{0.004})_2O_6$ (Jackson et al. 2003). Polarized IR spectral analyses of OEN from the same bulk sample indicates the presence of 70 ppm OH^- by weight (Skogby et al. 1990). Independent high-temperature (1 atm) Brillouin experiments were conducted with two scattering geometries: 80° symmetric scattering (platelet geometry), and 180° backscattering geometry. In the symmetric scattering geometry, sound velocities are obtained directly, whereas backscattering experiments yield the product of

*E-mail: jmjackso@uiuc.edu

refractive index and compressional-wave velocity, nV_P. All Brillouin measurements were performed using an Argon ion laser (λ = 514.5 nm) and a piezoelectrically scanned, 6-pass tandem Fabry-Perot interferometer (see Sinogeikin et al. 1998 for details). Inclusion-free single crystals were oriented and polished to a thickness of 150 and 300 μm, respectively. The symmetry and orientation of the samples were verified using x-ray diffraction before each Brillouin experiment.

For the symmetric scattering experiments, a (010) plate was loaded into a platinum holder and fixed using zirconia cement. No reaction was observed between the sample and cement during the experiment. The sample and holder were loaded into a high-temperature cell designed for symmetric scattering (Sinogeikin et al. 2000). The temperature was monitored using three thermocouples (two R-type and one K-type) adjacent to the sample. The maximum difference between the thermocouple measurements was 7 °C. Brillouin spectra were collected in ~100 °C increments from 23 to 800 °C, and in 25 °C increments to 1175 °C. All spectra in the symmetric scattering experiment were collected on increasing temperature. The sample was held at each temperature for about 2 h, with the total duration of ~48 h for this experiment.

For the backscattering experiments, an OEN plate with (001) surfaces was loaded without cement in a platinum envelope. This orientation was chosen because the symmetric scattering experiments indicated that the maximum elastic softening in the *a-c* plane occurs for the wave vector parallel to (001). A ceramic high-temperature furnace with a small optical aperture was used for backscattering measurements. This cell attains higher temperatures with smaller thermal gradients (Jackson et al. 2003), as compared with the cell designed for symmetric scattering. The platinum envelope and sample were attached to a ceramic tube and positioned in the center of the heating elements. The temperature was monitored by two R-type thermocouples on opposite sides of the sample. The maximum difference between the thermocouple measurements was 2 °C. Spectra were collected on increasing and decreasing temperature (Fig. 1). For the temperature interval 20 to 1000 °C, Brillouin spectra were collected in 100 °C increments with the sample being held at each temperature for ~30 min. Spectra were then collected in intervals of ~25 °C up to 1200 °C, with the sample being held at each temperature for ~20 min (Fig. 1a, temperature path 1). The temperature was decreased from 1200 to 1140 °C, and spectra were then collected every 10 min at 25 °C increments from 1140 to 1350 °C (Fig. 1b, temperature path 2) with clear indication of a phase transition to a higher temperature phase. The temperature was then decreased from 1350 to 1190 °C. Spectra were collected every ~50 °C from 1190 to 1000 °C, and every ~200 °C from 850 to 23 °C (Fig. 1c, temperature path 3), corresponding to a cooling rate of about 7°/min. The duration of the entire backscattering experiment was about 16 h. Orthoenstatite was verified as the recovered phase using a polarizing microscope and monochromatic XRD.

Results

The results from the backscattering and symmetric scattering experiments are shown in Figures 2a and 2b, respectively. In order to calculate the high-temperature, single-crystal elastic moduli, the density and, therefore, the volume thermal expansion is required. In a separate experiment, we determined the thermal expansion coefficient of OEN from the same bulk sample and obtained $\alpha(T) = 29.7(16) \times 10^{-6}\,\mathrm{K}^{-1} + 5.7(11) \times 10^{-9}\,\mathrm{K}^{-2}T$ (Jackson et al. 2003). Measurements of transverse and longitudinal velocities along [001] allowed the moduli C_{33} and C_{55} to be determined from the relationships $C_{55} = \rho V_{\mathrm{S},(001)}$ (polarization parallel to [100]), and $C_{33} = \rho V_{\mathrm{P},(001)}$, respectively. Within the uncertainties of the data, C_{33} and C_{55} exhibit a linearly decreasing trend with temperature up to about 900 °C (Fig. 3). At T > 900 °C, significant non-linear softening occurs in both moduli, which is a common type of pre-transitional behavior for displacive structural phase transitions (Pelous and Vacher 1976). In the temperature range from 20 to 1150 °C, C_{33} and C_{55} decrease by 52 and 31%, respectively.

From room temperature to 1350 °C, we observed only one phase transition on increasing temperature (Figs. 1 and 2). The transition occurred at 1175 °C in the symmetric scattering experiment and at 1250 °C in the backscattering experiment, which are in the middle-to-upper range of previously measured transition temperatures obtained for natural single-crystal OEN starting material (Fig. 4). Our observation is consistent with the study by Boysen et al. (1991) who observed only one transition on increasing temperature, but inconsistent with the studies of Brown and Smith (1963), Ernst and Schwab (1970), and Schrader et al. (1990), who reported intermediate phases or multiple phase transitions. Reid and Cohen (1967) described the Norton County (meteorite) OEN as having severely deformed and undeformed, as well as ordered and disordered regions occurring in the same crystal, perhaps explaining the large scatter in previous experiments on Norton OEN (Fig. 4). On decreasing temperature, the backscattering data are not

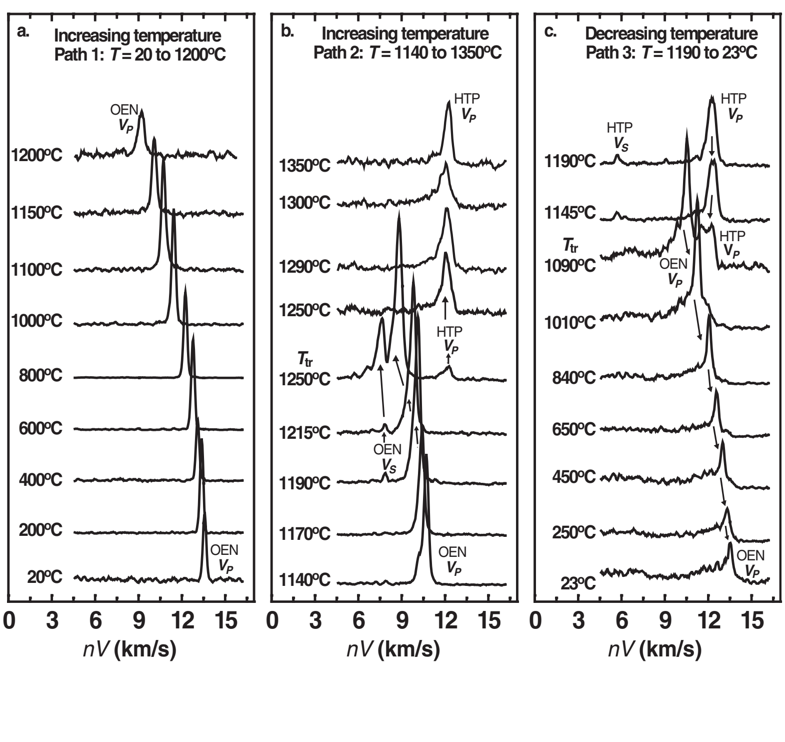

FIGURE 1. Selected Brillouin spectra from high-temperature backscattering measurements: (**a**) temperature path 1, heating; (**b**) temperature path 2, heating; (**c**) temperature path 3, cooling (see text for details). Coexistence of OEN and the high-temperature phase is observed at T_{tr} on increasing and decreasing temperature. Some intensity from shear modes results from the finite aperture of the optics. OEN = orthoenstatite, HTP = high-temperature phase.

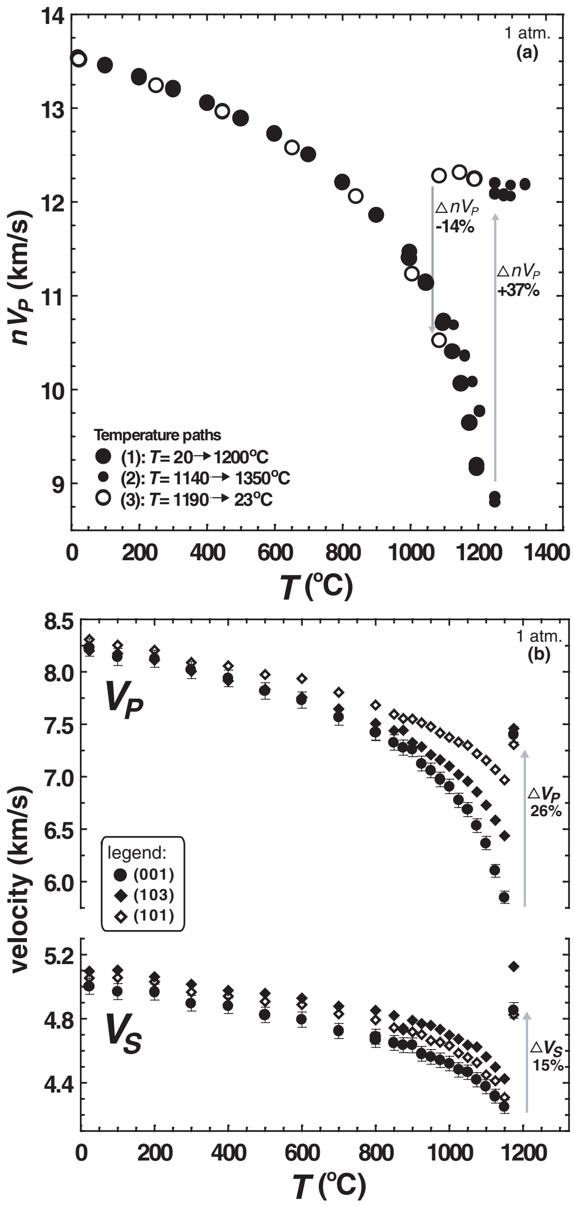

FIGURE 2. (**a**) The product of refractive-index (n) and compressional-wave velocity (V_P) (with wave vector approximately parallel to [001]) plotted as a function of temperature from backscattering measurements of single-crystal orthoenstatite. Temperature paths correspond to those in Figure 1. Errors are smaller than the size of the symbols. (**b**) Compressional (V_P) and shear (V_S) wave velocities in enstatite measured in three crystallographic directions as a function of increasing temperature from symmetric scattering measurements. All symbols correspond to crystallographic directions relative to OEN. Errors in velocity are the same for all crystallographic directions.

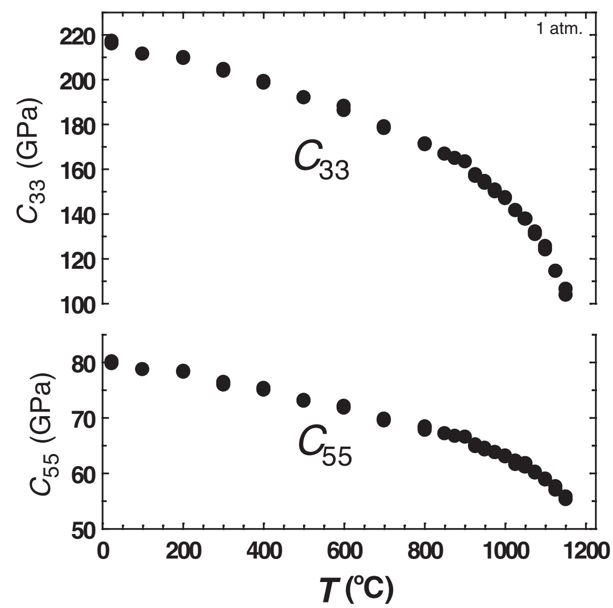

FIGURE 3. Single-crystal elastic moduli (C_{33} and C_{55}) for orthoenstatite as a function of temperature (see text for discussion). Errors are smaller than the size of the symbols.

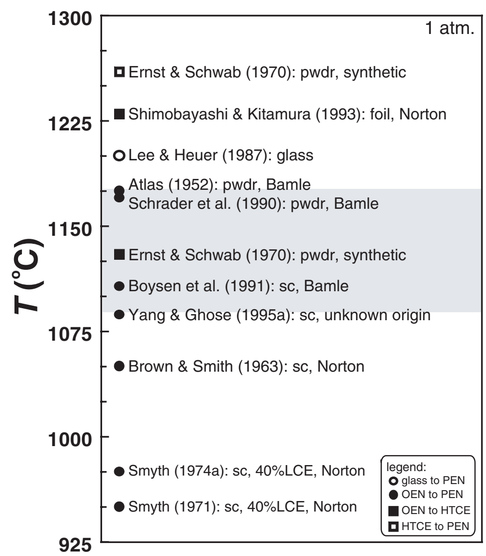

FIGURE 4. Phase transformations in $Mg_2Si_2O_6$ OEN to a higher-temperature polymorph (1 atm), as observed by various studies that used either natural or synthetic (no fluxes) OEN as starting material; all temperatures are taken from the first observation of the high-temperature phase on increasing temperature. Brief sample descriptions are cited adjacent to each reference; sc = single crystal, pwdr = powdered sample. The gray region defines the bracketed transition temperature from our study: 1090(10) °C ≤ T_{tr} ≤ 1175(10) °C.

inconsistent with the slight stiffening prior to the phase transition (T_{tr} = 1090 °C) observed by Boysen et al. (1991) using inelastic neutron scattering. At temperatures less than 1090 °C, our velocity measurements gave no indication of a second phase transition, for example to LCE, and OEN was verified as the recovered phase. The shape of the Brillouin peaks on decreasing temperature is different than on increasing temperature (Fig. 1), which we interpret to be caused by stacking disorder in OEN. By combining the results of the symmetric scattering and backscattering experiments, the transition temperature for OEN is: 1090(10) °C ≤ T_{tr} ≤ 1175(10) °C. The transformation is rapid (less than 10 minutes), rather than sluggish as suggested by previous XRD measurements (e.g., Yang and Ghose 1995a). Although LCE is proposed to be the stable low-temperature polymorph (Grover 1972), pressure and/or shear stresses may be necessary to stabilize LCE at ambient conditions (e.g., Kriven 1988). Our observations of a rapid transition to OEN upon cooling would appear to explain why OEN is the polymorph of $Mg_2Si_2O_6$ that is almost always seen in terrestrial rocks (Deer et al. 1978). Brillouin experiments do not provide direct structural information, so our results do not distinguish between PEN and HTCE as the high-temperature polymorph.

Discussion

Landau theory

The observed softening of C_{55} and C_{33} follows a pattern that is reminiscent of softening ahead of a displacive phase transition that is either tricritical (i.e., intermediate between first and second order) or just first order in character (Carpenter and Salje 1998, and references therein). *Pbca* is not a subgroup of either *Pbcn* or *C*2/*c*, with the implication that both *Pbca* ↔ *Pbcn* and *Pbca* ↔ *C*2/*c* transitions must necessarily be reconstructive. Therefore, the elastic softening could not be associated directly with either of the two phase transitions that are actually observed at Mg-rich and Fe-rich compositions. There are only two orthorhombic space groups of which *Pbca* is a subgroup, namely *Cmca* and *Ibca*. *Cmca* is more likely for a hypothetical high-temperature orthopyroxene structure because the relationship between *Cmca* and *Pbca* is closely analogous to the relationship between *C*2/*c* and $P2_1/c$, in that decreasing symmetry involves the loss of *C*-centering and a diad parallel to the crystallographic **b**-axis. Properties of the well-known $P2_1/c \leftrightarrow C2/c$ displacive transition in pigeonite and clinoenstatite thus provide a basis for predicting how the *Pbca* structure might behave at high temperatures in the absence of reconstructive transitions to the *Pbcn* or *C*2/*c* structures.

A transition *Pbca* ↔ *Cmca*, preserving the unit-cell size, has Y_2^+ as the active representation (using the notation of Stokes and Hatch 1988), and could be driven by a zone boundary soft mode. The Landau free energy expansion for this transition has the form:

$$G = \frac{1}{2}a\left(T - T_c\right)Q^2 + \frac{1}{4}bQ^4 + \frac{1}{6}cQ^6 + \lambda_1 e_1 Q^2 + \lambda_2 e_2 Q^2 + \lambda_3 e_3 Q^2 + \lambda_4 e_4^2 Q^2 + \lambda_5 e_5^2 Q^2 + \lambda_6 e_6^2 Q^2 + \frac{1}{2}\sum_{i,k=1-3} C_{ik}^o e_i e_k + \frac{1}{2}\sum_{i=4-6} C_{ii}^o e_i^2 \tag{1}$$

where Q is the order parameter, T_c is the critical temperature, a, b, and c are normal Landau coefficients, λ_1-λ_6 are coupling coefficients, e_1-e_6 are strains ($e_1 \neq e_2 \neq e_3 \neq 0$, $e_4 = e_5 = e_6 = 0$), and C_{ik}^0 are elastic constants of the *Cmca* structure. In its renormalized form, this expansion becomes:

$$G = \frac{1}{2}a\left(T - T_c\right)Q^2 + \frac{1}{4}b^*Q^4 + \frac{1}{6}cQ^6 \tag{2}$$

where b^* includes the effects of strain/order parameter coupling, with strain being proportional to Q^2. If it is assumed that the transition is tricritical in character ($b^* = 0$), the solution for Q as a function of temperature becomes:

$$Q^4 = \frac{a}{c}\left(T_c - T\right) = \left(\frac{T_c - T}{T_c}\right) \tag{3}$$

and the transition occurs at $T = T_c$. C_{55} for the *Pbca* structure is then expected to vary as

$$C_{55} = C_{55}^o + 2\lambda_5 Q^2 = C_{55}^o + 2\lambda_5\left(\frac{T_c - T}{T_c}\right)^{1/2}. \tag{4}$$

The variation of C_{33} is derived from the usual relationship (Slonsczewski and Thomas 1970):

$$C_{ik} = C_{ik}^o - \sum_{m,n} \frac{\partial^2 G}{\partial e_i \partial Q_m}\left(\frac{\partial^2 G}{\partial Q_m \partial Q_n}\right)^{-1} \frac{\partial^2 G}{\partial e_k \partial Q_n} \tag{5}$$

which gives

$$C_{33} = C_{33}^o - 4\lambda_3^2 Q^2 \cdot \left(\frac{\partial^2 G}{\partial Q^2}\right)^{-1}. \tag{6}$$

From Equation 1:

$$\begin{aligned}\frac{\partial^2 G}{\partial Q^2} &= a\left(T - T_c\right) + 3bQ^2 + 5cQ^4 + 2\lambda_1 e_1 + 2\lambda_2 e_2 + 2\lambda_3 e_3 \\ &= a\left(T - T_c\right) + \left(2b + b^*\right)Q^2 + 5cQ^4\end{aligned} \tag{7}$$

(see also Carpenter et al. 2003). Substituting the equilibrium solution for Q (Eq. 3), with $b^* = 0$, gives:

$$\frac{\partial^2 G}{\partial Q^2} = 4a\left(T_c - T\right) + 2bQ^2 \tag{8}$$

and, hence:

$$C_{33} = C_{33}^o - \frac{4\lambda_3^2}{4cQ^2 + 2b}. \tag{9}$$

Numerical values are not available either for the bare elastic constants or for any of the coefficients in Equation 1, but Equations 3, 4, and 9 at least give the form of temperature dependence expected for C_{33} and C_{55}, (illustrated in Figure 5 for more-or-less) arbitrary values of the coefficients. Note that if the transitions were just first order ($b^* < 0$), the patterns for C_{33} and C_{55} would still be similar to those shown in Figure 5, but the transition would occur at a temperature T_{tr}, with $T_{tr} > T_c$, and there would be discontinuities in both C_{33} and C_{55} at $T = T_{tr}$. Note that C_{33} is predicted to have a different temperature dependence from C_{55}, as appears to be the case in the observed variations shown in Figure 3.

Analogies with the pyroxene *C*2/*c* ↔ $P2_1/c$ transition

The $C2/c \leftrightarrow P2_1/c$ transition in pigeonite and clinoenstatite occurs by rotations of tetrahedra within the pyroxene chains, to give a change in coordination around the M2 cation site. There are close structural similarities between the *Pbca* and $P2_1/c$ structures, in that the former is effectively alternating (100) twins of the latter on a unit-cell scale (see, for example, Boysen et al. 1991, and references therein). The pattern of non-linear variations of tetrahedral chain rotation angles with temperature in the $P2_1/c$ structure, which gives rise to the change in coordination at the M2 site (Brown et al. 1972; Smyth 1974b; Pannhorst 1984; Arlt and Armbruster 1997; Cámara et al. 2002), is also displayed by orthopyroxenes (Smyth 1973; Sueno et al. 1976, 1984; Yang and Ghose 1995a, 1995b). In $P2_1/c$ structures, the rotation angles of the A and B chains converge, becoming identical in the *C*2/*c* structure. The difference in rotation angles thus reflects the variation of the order parameter for the $C2/c \leftrightarrow P2_1/c$ transition. The same convergence occurs in *Pbca* structures and, as already discussed by Yang and Ghose (1995b), the difference in chain angles also has the characteristic

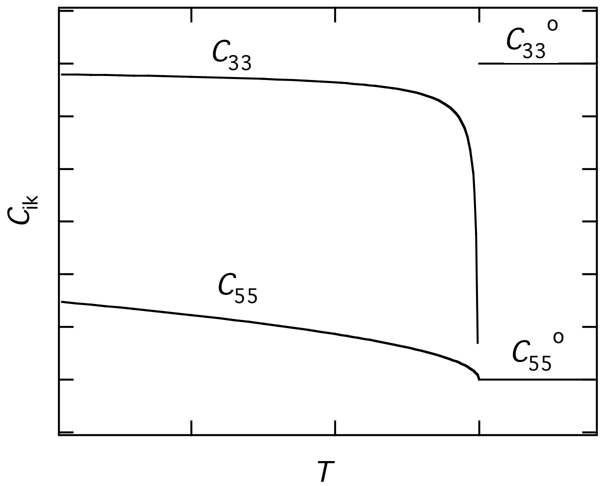

FIGURE 5. Predicted pattern of variations for C_{33} and C_{55} due to a *Cmca* ↔ *Pbca* transition described by Equation 1. The elastic constants were calculated using Equations 4 and 9 with more-or-less arbitrary values for the coefficients.

evolution of an order parameter. It is proposed here that the difference in chain angles would be the order parameter for the transition *Cmca* ↔ *Pbca*. By analogy with the structural relationships between $P2_1/c$ and *Pbca* pyroxenes, a *Cmca* pyroxene might be a unit-cell-scale twinned version of $C2/c$ pyroxene, containing only one symmetrically distinct tetrahedral chain.

The transition temperature for the $C2/c \leftrightarrow P2_1/c$ transition decreases with increasing Ca and Fe content in pigeonite (Prewitt et al. 1971; Arlt et al. 2000). The thermodynamic character also changes from first order in Fe-free crystals (Tribaudino et al. 2002) to close to tricritical (2-4-6 Landau potential) in crystals with composition ~$En_{47}Fs_{43}Wo_{10}$ (Cámara et al. 2002, 2003). In this context, it is interesting to note that the chain rotation angles converge almost continuously at ~1000 °C in orthoferrosilite (Sueno et al. 1976), but show a much smaller convergence by ~1100 °C in orthoenstatite. Perhaps the *Cmca* ↔ *Pbca* transition also would be first order (but close to tricritical) in Fe-free crystals. These temperatures are above the $C2/c \rightarrow P2_1/c$ transition temperature but the effect of Fe ↔ Mg substitution on the transition temperature appears to be qualitatively the same. Finally, if there are acoustic anomalies associated with a displacive phase transition, there also must be strain anomalies. In the present case (Eq. 1), the elastic softening of C_{33} and C_{55} is being interpreted as arising from coupling of the strains e_3 and e_5 with the driving order parameter, Q. Coupling of the form $\lambda e_3 Q^2$ leads to the relationship $e_3 \propto Q^2$ and, for a tricritical transition, e_3 is thus expected to vary as $e_3^2 \propto T$. This form of coupling should appear in the lattice parameters as a strongly non-linear temperature dependence for c. The lattice parameters of pigeonite and clinoenstatite show markedly non-linear variations with temperature (Smyth 1974b; Pannhorst 1984; Tribaudino et al. 2002; Cámara et al. 2002, 2003) and similar patterns are observed in orthopyroxene (Smyth 1973; Sueno et al. 1976; Yang and Ghose 1995a, 1995b; Jackson et al. 2003). In particular, a and c display a concave upward pattern whereas b is usually concave downward. These variations can sensibly be interpreted in terms of order parameter coupling with each of e_1, e_2, and e_3, with the consequence that elastic anomalies should be expected for C_{11}, C_{22}, C_{33}, C_{12}, C_{13}, and C_{23} in both $P2_1/c$ and *Pbca* pyroxene crystals.

Relationship of the *Cmca* ↔ *Pbca* transition to the *Pbcn* ↔ *Pbca* and *C2/c* ↔ *Pbca* transitions

Elastic softening in *Pbca* enstatite might be indicative of a displacive transition at high temperatures, but the transition that actually occurs is reconstructive, *Pbca* → *Pbcn* (or *Pbca* → $C2/c$). At Fe-richer compositions, the transition is *Pbca* → $C2/c$ (Smyth 1969; Sueno et al. 1976). The proposed *Cmca* structure does not appear to have an equilibrium field of stability at any pressure-temperature range so far investigated. This feature, however, does not mean that the transitions are unrelated. In particular, the steep decrease of C_{33} described here suggests that the *Cmca* ↔ *Pbca* transition temperature is not far above ~1150 °C (compare Figs. 3 and 5). Schematic free energy curves consistent with our above interpretation are shown in Figs. 6. The *Cmca* structure is shown as being unstable with respect to *Pbcn* at all temperatures. Lowering of the free energy due to the *Cmca* ↔ *Pbca* transition, by an amount given by Equation 1, causes the *Pbca* structure to become more stable than the *Pbcn* structure at low temperatures. If the free energy difference between *Cmca* and *Pbcn* structures is small, the difference in temperature between the two transitions (labeled T_1 and T_2 in Fig. 6) will also be small.

In addition to the issue of thermodynamic stability, the elastic softening might enhance the kinetics of the reconstructive *Pbca* → *Pbcn* (or *Pbca* → $C2/c$) transition. As the crystals become elastically soft, they will become progressively more sensitive to externally applied stresses. Thus the observed behavior of orthopyroxenes may represent a rather rare example of a material in which a displacive phase transition to one structure actually triggers a reconstructive transition to a quite different structure. Furthermore, the elastic softening observed in orthoenstatite could have important implications for Earth's upper mantle.

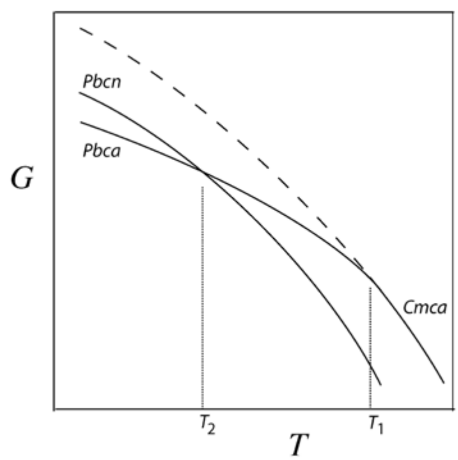

FIGURE 6. Schematic free energy curves to illustrate a possible relationship between *Pbca*, *Pbcn,* and *Cmca* structures of enstatite. A displacive *Cmca* ↔ *Pbca* transition is shown as occurring at T_1 and a reconstructive *Pbca* ↔ *Pbcn* transition at T_2. The *Cmca* structure is shown as being unstable with respect to the *Pbca* structure below T_1 (solid line, extrapolated below T_1 as a dashed line) and to the *Pbcn* structure at all temperatures.

ACKNOWLEDGMENTS

We thank George Rossman (California Institute of Technology) for providing the orthoenstatite samples (GRR 649, AMNH 100634), Ian Steele (University of Chicago) for assistance with the microprobe analyses, and Scott Wilson (UIUC) for the XRD analyses. We are also grateful to Charlie Prewitt, Bruno Reynard, Philippe Gillet, Ross Angel, Wolfgang Sturhahn, Holger Hellwig, Donald Lindsley, and Dmitry Lakshtanov for helpful discussions. Richard Harrison and Ross Angel are thanked for their helpful reviews.

REFERENCES CITED

Angel, R.J., Chopelas, A., and Ross, N.L. (1992) Stability of high-density clinoenstatite at upper-mantle pressures. Nature, 358, 322–324.

Arlt, T. and Armbruster, T. (1997) The temperature-dependent $P2_1/c$-$C2/c$ phase transition in the clinopyroxene kanoite $MnMg[Si_2O_6]$: a single-crystal X-ray and optical study. European Journal of Mineralogy, 9, 953–964.

Arlt, T., Kunz, M., Stolz, J., Armbruster, T., and Angel, R.J. (2000) *P-T-X* data on $P2_1/c$-clinopyroxenes and their displacive phase transitions. Contributions to Mineralogy and Petrology, 138, 35–45.

Atlas, L. (1952) The polymorphism of $MgSiO_3$ and solid-state equilibria in the system $MgSiO_3$-$CaMgSi_2O_6$. Journal of Geology, 60, 125–147.

Biggar, G.M. (1992) Subsolidus equilibria between protopyroxene, orthopyroxene, pigeonite and diopside, in the $MgSiO_3$-$CaMgSi_2O_6$ at 1 bar to 9.5 kbar, and 1012 to 1450°C. European Journal of Mineralogy, 4, 153–170.

Boyd, F.R., England, J.L., and Davis, B.T.C. (1964) Effects of pressure on the melting and polymorphism of enstatite, $MgSiO_3$. Journal of Geophysical Research, 69, 2101–2109.

Boysen, H., Frey, F., Schrader, H., and Eckold, G. (1991) On the proto- to ortho- /clino enstatite phase transformation: single crystal X-ray and inelastic neutron investigation. Physics and Chemistry of Minerals, 17, 629–635.

Bozhilov, K.N., Green, II H.W., and Dobrzhinetskaya, L. (1999) Clinoenstatite in Alpe Arami peridotite: additional evidence of very high pressure. Science, 284, 128–132.

Brown, W.L. and Smith, J.V. (1963) High-temperature X-ray studies on the polymorphism of $MgSiO_3$. Zeitschrift für Kristallographie, 118, 186–212.

Brown, G.E., Prewitt, C.T., Papike, J.J., and Sueno, S. (1972) A comparison of the structures of low and high pigeonite. Journal of Geophysical Research, 77, 5778–5780.

Busek, P.R. and Iijima, S. (1975) High resolution electron microscopy of enstatite: II: Geological applications. American Mineralogist, 60, 771–784.

Cámara, F., Carpenter, M.A., Domeneghetti, M.C., and Tazzoli, V. (2002) Non-convergent ordering and displacive phase transition in pigeonite: in situ HT XRD study. Physics and Chemistry of Minerals, 29, 331–340.

———(2003) Coupling between non-convergent ordering and transition temperature in the $C2/c \leftrightarrow P2_1/c$ phase transition in pigeonite. American Mineralogist, 88, 1115–1128.

Carpenter, M.A. and Salje, E.K.H. (1998) Elastic anomalies in minerals due to structural phase transitions. European Journal of Mineralogy, 10, 693–812.

Carpenter, M.A., Meyer, H.-W., Sondergeld, P., Marion, S., and Knight, K.S. (2003) Spontaneous strain variations through the low temperature phase transitions of deuterated lawsonite. American Mineralogist, 88, 534–546.

Choudhury, N. and Chaplot, S.L. (2000) Free energy and relative stability of the enstatite $Mg_2Si_2O_6$ polymorphs. Solid State Communications, 114, 127–132.

Choudhury, N., Ghose, S., Pal Chowdhury, C., Loong, C.K., and Chaplot, S.L. (1998) Lattice dynamics, Raman spectroscopy, and inelastic neutron scattering of orthoenstatite $Mg_2Si_2O_6$. Physical Review B, 58, 756–765.

Deer, W.A., Howie, R.A., and Zussman, J. (1978) Rock-forming minerals: Single-chain silicates. Wiley, New York.

Ernst, T. and Schwab, R. (1970) Stability and structural relations of (Mg,Fe) metasilicates. Physics of the Earth and Planetary Interiors, 3, 451–455.

Grover, J. (1972) Two problems in pyroxene mineralogy: A theory of partitioning of cations between coexisting single- and multi- site phases and a determination of the stability of low-clinoenstatite under hydrostatic pressure. PhD thesis, Yale University.

Iishi, K. and Kitayama, H. (1995) Stability of high clinoenstatite. Neues Jahrbuch für Mineralogie Monatsh, 2, 65–74.

Jackson, J.M., Palko, J.W., Andrault, D., Sinogeikin, S.V., Lakshtanov, D.L., Wang, J., Bass, J.D., and Zha C-S. (2003) Thermal expansion of natural orthoenstatite to 1473 K, European Journal of Mineralogy, 15, 469–473.

Jiang, D., Fujino, K, Tomioka, N., Hosoya, T., and Das, K. (2002) High-temperature X-ray diffraction study of enstatite up to the melting point. Journal of Mineralogical and Petrological Sciences, 97, 20–31.

Komatsu, M. (1980) Clinoenstatite in volcanic rocks from the Bonin Islands. Contributions to Mineralogy and Petrology, 74, 329–338.

Kriven, W.M. (1988) Possible alternative transformation tougheners to zirconia: crystallographic aspects. Journal of the America Ceramic Society, 71, 1021–1030.

Kurat, G., Palme, H., Embey-Isztin, A., Touret, J., Ntaflos, T., Spettel, B., Brandstatter, F., Palme, C., Dreibus, G., and Prinz, M. (1993) Petrology and geochemistry of peridotites and associated vein rocks of Zabargad Island, Red Sea, Egypt. Mineralogy and Petrology, 48, 309–341.

Lee, W.E. and Heuer, A.H. (1987) On the polymorphism of enstatite. Journal of American Ceramic Society, 70, 349–360.

Matsui, M. and Price, G.D. (1992) Computer simulation of the $MgSiO_3$ polymorphs. Physics and Chemistry of Minerals, 18, 365–372.

Murakami, T., Taleuchi, Y., and Yamanaka, T. (1982) The transition of orthoenstatite to protoenstatite and the structure at 1080°C. Zeitschrift für Kristallographie, 160, 299–312.

Pannhorst, W. (1984) High temperature crystal structure refinements of low-clinoenstatite up to 700 °C. Neues Jahrbuch für Mineralogie Abhandlungen, 150, 219–228.

Pelous, J. and Vacher, R. (1976) Thermal Brillouin scattering in crystalline and fused quartz from 20 to 1000°C. Solid State Communications, 18, 657–661.

Prewitt, C.T., Brown, G.E., and Papike, J.J. (1971) Apollo 12 clinopyroxenes: high temperature X-ray diffraction studies. Proceedings of the Second Lunar Science Conference, 1, 59–68.

Reid, A.M. and Cohen, A.J. (1967) Some characteristics of enstatite from enstatite achondrites. Geochimica et Cosmochimica Acta, 31, 661–672.

Ross, N.L. and Reynard, B. (1999) The effect of iron on the $P2_1/c$ to $C2/c$ transition in $(Mg,Fe)SiO_3$ clinopyroxenes. European Journal of Mineralogy, 11, 585–589.

Sarver, J.F. and Hummel, F.A. (1962) Stability relations of magnesium metasilicate polymorphs. Journal of American Ceramic Society, 45, 152–156.

Schrader, H., Boysen, H., Frey, F., and Convert, P. (1990) On the phase transformation proto- to clino/orthoenstatite: Neutron powder investigation. Physics and Chemistry of Minerals, 17, 409–415.

Shimobayashi, N. and Kitamura, M. (1991) Phase transition in Ca-poor clinopyroxenes. Physics and Chemistry of Minerals, 18, 153–160.

———(1993) Phase transition of orthoenstatite to high-clinoenstatite: in situ TEM study at high temperatures. Mineralogical Journal, 16, 416–426.

Sinogeikin, S.V., Katsura, T., and Bass, J.D. (1998) Sound velocities and elastic properties of Fe-bearing wadsleyite and ringwoodite. Journal of Geophysical Research, 103, B9, 20819–20825.

Sinogeikin, S.V., Jackson, J.M., O'Neill, B., Palko, J., and Bass, J.D. (2000) Compact high-temperature cell for Brillouin scattering measurements. Review of Scientific Instruments, 71, 201–206.

Skogby, H., Bell, D.R., and Rossman, G.R. (1990) Hydroxide in pyroxene: variations in the natural environment. American Mineralogist, 75, 764–774.

Slonczewski, J.C. and Thomas, H. (1970) Interaction of elastic strain with the structural transition of strontium titanate. Physical Review B, 1, 3599–3608.

Smyth, J.R. (1969) Orthopyroxene-high-low clinopyroxene inversions. Earth and Planetary Science Letters, 6, 406–407.

———(1971) Protoenstatite: a crystal-structure refinement at 1100°C. Zeitschrift für Kristallographie, 134, 262–274.

———(1973) An orthopyroxene structure up to 850 °C. American Mineralogist, 58, 636–648.

———(1974a) Experimental study of the polymorphism of enstatite. American Mineralogist, 59, 345–352.

———(1974b) The high temperature crystal chemistry of clinohypersthene. American Mineralogist, 59, 1069–1082.

Stokes, H.T. and Hatch, D.M. (1988) Isotropy subgroups of the 230 crystallographic space groups. World Scientific, Singapore.

Sueno, S. and Prewitt, C.T. (1983) Models for the phase transition between orthoferrosilite and high clinoferrosilite. Fortschritte der Mineralogie, 61, 223–241.

Sueno, S., Cameron, M., and Prewitt, C.T. (1976) Orthoferrosilite: high temperature crystal chemistry. American Mineralogist, 61, 38–53.

Sueno, S., Kimata, M., and Prewitt, C.T. (1984) The crystal chemistry of high clinoferrosilite. American Mineralogist, 69, 264–269.

Thiéblot, L., Téqui, C., and Richet, P. (1999) High-temperature heat capacity of grossular ($Ca_3Al_2Si_3O_{12}$), enstatite ($MgSiO_3$), and titanite ($CaTiSiO_5$). American Mineralogist, 84, 848–855.

Tribaudino, M., Nestola, F., Cámara, F., and Domeneghetti, M.C. (2002) The high-temperature $P2_1/c$-$C2/c$ phase transition in Fe-free pyroxene ($Ca_{0.15}Mg_{1.85}Si_2O_6$): structural and thermodynamic behavior. American Mineralogist, 87, 648–657.

Ulmer, P. and Stalder, R. (2001) The $Mg(Fe)SiO_3$ orthoenstatite-clinoenstatite transitions at high pressures and temperatures determined by Raman-spectroscopy on quenched samples. American Mineralogist, 86, 1267–1274.

Yang, H. and Ghose, S. (1995a) High temperature single crystal X-ray diffraction studies of the ortho-proto phase transition in enstatite, $Mg_2Si_2O_6$ at 1360 K. Physics and Chemistry of Minerals, 22, 300–310.

———(1995b) A transitional structural state and anomalous Fe-Mg order-disorder in Mg-rich orthopyroxene, $(Mg_{0.75}Fe_{0.25})Si_2O_6$. American Mineralogist, 80, 9–20.

MANUSCRIPT RECEIVED MAY 16, 2003
MANUSCRIPT ACCEPTED AUGUST 19, 2003
MANUSCRIPT HANDLED BY SIMON KOHN